Adaptation of Orienting Behavior: From the Barn Owl to a Robotic System

Michele Rucci, *Member, IEEE,* Gerald M. Edelman, and Jonathan Wray

***Abstract*— Autonomous robotic systems need to adjust their sensorimotor coordinations so as to maintain good performance in the presence of changes in their sensory and motor characteristics. Biological systems are able to adapt to large variations in their physical and functional properties. In the last decade, the adjustment of orienting behavior has been carefully investigated in the barn owl, a nocturnal predator with highly developed auditory capabilities. We have recently proposed that the development and maintenance of the barn owl's accurate orienting behavior can be explained through a process of learning based on the saliency of sensorimotor events. In this paper we consider the application of a detailed computer model of the principal neural structures involved in the process of spatial localization in the barn owl to the control of the orienting behavior of a robotic system, in the presence of auditory and visual stimulation. The system is composed of a robotic head equipped with two lateral microphones and a camera. We show that the model produces accurate orienting behavior toward both auditory and visual targets and is able to quickly recover good performance after alterations of the sensory inputs and motor outputs. The results illustrate that an architecture specifically designed to account for biological phenomena can produce flexible and robust motor control of a robotic system operating in the real world.**

***Index Terms*—Adaptive control, autonomous calibration, neural networks, spatial localization.**

I. Introduction

THE variability of the world presents a major challenge to researchers involved in the development of autonomous robotic systems. These systems need to possess a high degree of flexibility in order to adapt to the continuously changing conditions of the environment and of their own sensors and motors. In the course of evolution, nature has faced the very same problems engineers and computer scientists are currently encountering. As a result of millions of years of natural selection, systems have emerged that are highly flexible in the face of variable phenotypic and environmental conditions.

Although there is no doubt that the understanding of the basic principles of how brains operate and adapt to the environment will lead to a major revolution in the design of artificial systems, and despite the existence of many problems common to both robotics and neuroscience, so far only occasional interaction has occurred between these two fields (see for example [1]–[4]). Recently, neuroscientists have turned to the use of robotic systems as a way to quantitatively test and analyze theories that would otherwise remain speculative. According to the approach of synthetic neural modeling (SNM) [5], [6], theoretical neural principles are investigated by coupling computational models of brain structures with systems interacting in the real world. This approach differs from connectionist approaches (see, for reviews, [7], [8]) in its degree of biological realism, and arises from the need to simultaneously examine multiple brain regions and various levels of control in freely behaving animals over long periods of time. This is an operation that, although crucial to the comprehension of how brain function and behavior interact, is currently not feasible *in vivo* due to technical limitations. SNM establishes a direct link between the neurosciences and engineering that, while providing neuroscientists with new insights into the functioning of neural systems, can offer new ideas to researchers in AI and robotics.

In this paper, by focusing on the case of adaptation of orienting behavior, we provide an example of how an architecture specifically designed to replicate a biological system can produce robust and flexible motor control of a robotic system. The system that we describe is based on a model of some neural structures in the brain of the barn owl. It is able to orient toward auditory and visual targets and maintain accurate performance in the face of drastic sensorimotor manipulations. This provides one of the earliest examples of a robotic system efficiently controlled by an accurate model of specific structures of the brain.

A. Orienting Behavior in Robotic Systems

Orienting behavior is the motor action by which visual sensors are redirected toward a target. In the presence of sensors with anisotropic resolution similar to eyes of vertebrates [9], orienting behavior allows the examination of the target with the fovea, the region at the center of the visual field with highest spatial acuity. Orienting behavior is also important with uniform resolution sensors (see [10] for a review), as it permits visual analysis of stimuli detected by other sensory modalities. It also allows the allocation of the available computational resources to a selected region of the image, an important step toward the goal of achieving real-time performance [11], [12]. In addition, as emphasized by research in the field of computer vision, features of the visual scene which are ambiguous in single views can be recovered by controlling the direction of gaze [13]–[15]. Since targets

Manuscript received November 7, 1997; revised June 15, 1998. This paper was supported in part by the van Ameringen Foundation, Novartis Pharmaceutical Corporation, and the Theoretical Neurobiology Program, The Neurosciences Institute, Neurosciences Research Foundation. This paper was recommended for publication by Associate Editor I. Walker and Editor V. Lumelsky upon evaluation of the reviewers' comments.

The authors are with The Neurosciences Institute, San Diego, CA 92121 USA.

Publisher Item Identifier S 1042-296X(99)00989-1.

may be perceived in any of the available sensory modalities, redirecting the direction of gaze is not a trivial operation. Different sensory inputs are represented in different manners, as in activation of receptors of the eyes or cameras for vision or in detection of spectral components of sound for audition. In all cases, coordinate transformations are required to convert sensory stimuli into corresponding motor outputs. These transformations depend on the structure and characteristics of the system under consideration, and they need to be tuned to compensate for changes in the components of the system.

Calibration is a well-known procedure for evaluating transformation matrices, and has been widely used with head-eye (or hand-eye) systems to determine the relations between image and motor coordinates [16]–[20]. Unfortunately, calibration procedures often require the use of calibrating tools and the interruption of the normal functioning of the system, an operation which may not be feasible in specific applications. In the last few years, within the framework of visual servoing [21], [22], examples have been provided of systems that operate efficiently even in the absence of accurate calibrations [23]–[27]. In particular, methods of self-calibration have been proposed that find the elements of the appropriate transformation matrices by analyzing changes in the input image during measured movements [28]–[33]. These approaches do not require the use of calibrating tools and are more suited for autonomous systems operating in unstructured environments. Moreover, in some of these methods calibration parameters can be updated continuously while the system is executing other tasks. However, the extension of such techniques to input modalities other than vision is not immediately obvious. For example, it is not clear how they could be applied to cases in which input signals are not passively propagated through the environment, as is the case with touch [34], or when signals are not explicitly spatially organized, as in the auditory domain.

B. Spatial Localization and Orienting Behavior in the Barn Owl

In the last two decades, neuroscientists have carefully investigated the process of spatial localization and orienting behavior in the barn owl, a nocturnal predator with accurate visual and auditory capabilities [35]. As with many other species, there is little doubt that the barn owl learns to orient toward targets on the basis of sensorimotor experience. During growth, its body changes significantly in size and shape, and its brain must constantly tune sensorimotor coordinations in order to ensure accurate localization. This is particularly evident in the case of auditory localization. Behavioral experiments have shown that, unlike humans, barn owls rely on two separate auditory cues for the localization of the azimuth and elevation of a sound source: differences in the time of arrival of the sounds at the two ears [interaural time differences (ITD's)] are used for localizing the azimuth, and differences in amplitudes [interaural level differences (ILD's)] are used for the elevation (see [36] for a review). While the same basic cues for auditory localization are used by all barn owls, their actual values have been found to vary significantly among and within individuals, because they depend on the size of the head and the shape of the facial ruff of feathers. As these morphological features change during growth, auditory localization must be continuously tuned to compensate for corresponding changes in cue values.

Fig. 1(a) schematically illustrates some of the structures in the brain of the barn owl involved in spatial localization. Two separate neural pathways process auditory and visual inputs and converge in the optic tectum (OT). The OT, the equivalent of the superior colliculus in mammals [37], is a structure well known to be involved in the production of orienting behavior. Within the auditory pathway, physiological investigations have shown the existence of two separate parallel neural pathways specialized for the independent analysis of ITD's and ILD's [38]. These pathways converge at the level of the inferior colliculus, an auditory nucleus that projects to the OT. Neurophysiological investigations have established that neurons in the OT respond to visual and auditory cues positioned in specific regions of the owl's surrounding space [39]. In addition, it has been observed that stimulation of OT neurons produces movements of the head in specific directions [40]. The spatial regions in which visual and auditory stimuli activate a cell in the OT are usually referred to as the visual and auditory receptive fields (RF's) of the neuron, and the mean direction of gaze elicited by micro-stimulations define the so-called motor RF of the cell. It has been found that in the OT of normal barn owls, cells are spatially arranged so that the layout of their RF's gives rise to auditory, visual and motor maps of external space [39]. In addition, these maps of space are usually found in close alignment with each other [41]. That is, OT neurons are activated by sound sources at spatial locations corresponding to the cells' visual RF's, and elicit movements of the head toward these same locations. In this way, the perceived position of a stimulus is converted into a corresponding movement which orients the head and the eyes toward the target.

In order to understand the mechanisms underlying learning and adaptation of orienting behavior, experiments involving manipulations of the sensory inputs have shown that young barn owls are able to adapt to drastic alterations of their sensory conditions [42]. These experiments have also revealed a neural correlate of the adaptation of orienting behavior in the reacquisition of alignment between sensory and motor maps in the OT [43]–[45]. Analysis of the brains of barn owls raised in the presence of chronically altered sensory conditions have led to the identification of specific sites in which neurons change their patterns of connectivity on the basis of sensorimotor experience [46], [47]. These modifications are responsible for the readjustment of visual, auditory and motor RF's in the OT.

Based on a careful study of the barn owl literature, as well as on a large body of biological evidence in different species, we have recently proposed [48] that the development and maintenance of accurate spatial localization can be explained in the context of a neurobiologically-based paradigm of reinforcement learning [49], [50], which we call *value-dependent learning* [6], [51]. According to this paradigm, signals related to the saliency of sensory and motor events are broadcast by diffuse projecting systems to many parts of the brain, where they modulate changes in the strengths of connections

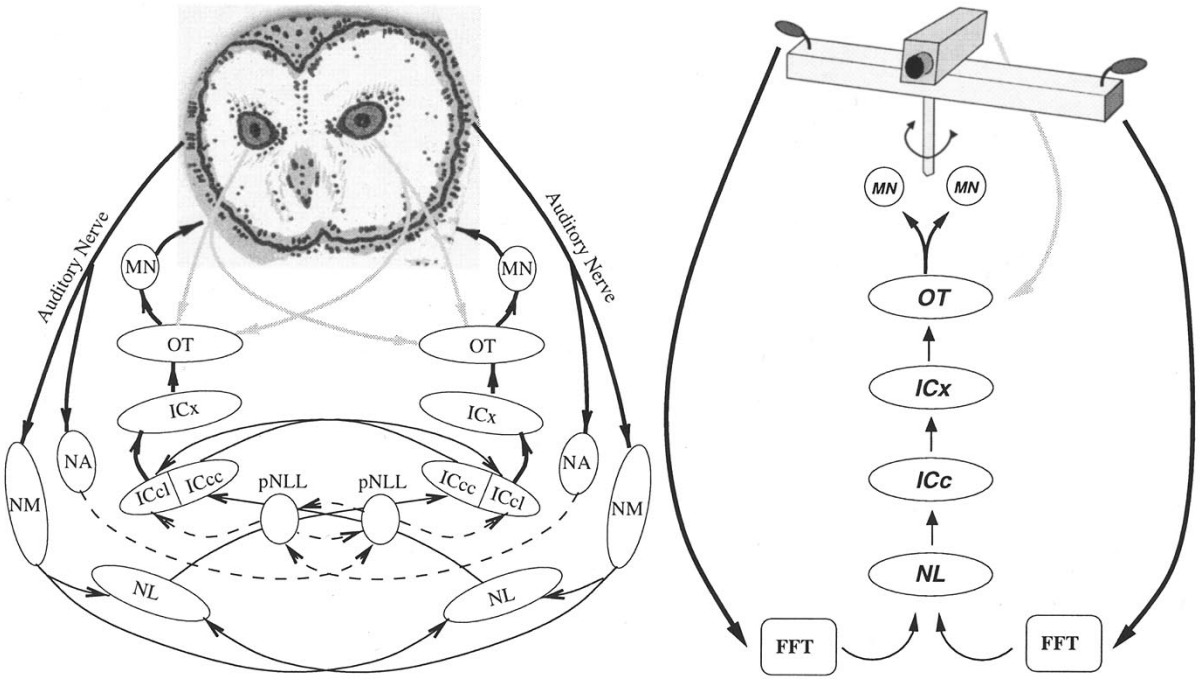

(a) (b)

Fig. 1. The main neural structures involved in spatial localization in the barn owl and the modeled system. (a) In the brain of the barn owl, similarly to the brain of many other species, projections from visual and auditory structures converge in the optic tectum (OT), which, in turn, projects to motor nuclei (MN) that control the movement of the head. The visual pathway (grey arrows) is composed of direct projections from the retina to the OT. Within the auditory pathway (black arrows) different structures are specialized for processing ITD's and ILD's. These two separate pathways converge at the level of the internal nucleus of the inferior colliculus (ICc), which projects to the external nucleus (ICx) and from there to the OT. The ILD pathway (dashed arrows) includes the nucleus angularis (NA) and the posterior lateral lemniscal nucleus (pNLL). The ITD pathway (solid arrows) includes the nucleus magnocellularis (NM) and the nucleus laminaris (NL). (b) The robotic system considered in this paper was composed of a mobile head equipped with two microphones and a camera. Movements along the pan axis of the head were controlled by a model of the owl structures involved in the localization of the azimuth. Both the visual and ITD auditory pathways to the OT were included (see text for details).

among neurons. The proposal that the adaptation of orienting behavior occurs through a mechanism of value-dependent learning does not require biologically unrealistic computations and is consistent with what is presently known about the neuroanatomical organization of the auditory pathways to the OT in the barn owl. This hypothesis is supported by the results of simulations of a computer model of the neural structures involved in the generation of orienting behavior in the owl, which are in agreement with a wide range of physiological data [48].

In the present paper, we consider the application of a more complete version of this model to the control of the direction of gaze of a robotic platform, in the presence of both auditory and visual stimulation. The system that we consider is schematically illustrated in Fig. 1(b). A robotic head equipped with a camera and two microphones is controlled by a computer model of the neural pathways of the barn owl involved in the localization of the azimuth. Adaptation in the model is achieved by allowing synaptic modifications to occur in those structures which have been observed to be plastic in the barn owl. According to the proposed learning scheme, synaptic strengths in the model were influenced by the activity of a diffuse projecting modulatory system which signaled the occurrence of behaviorally salient events, such as successful foveation. We show that, independent of the characteristics and the precise relative arrangements of the components of the robot, the model develops accurate and robust localization in the presence of different sensorimotor conditions, and quickly recovers good performance after manipulations of sensory and motor characteristics.

In the following section, we describe in detail how the main brain structures of the owl involved in spatial localization have been modeled. In Section III, we present the results of the application of the model to the control of the robotic system. Finally, a brief discussion is included in Section IV.

II. Modeling the Barn Owl Nervous System

As illustrated in more detail in Fig. 2, the model described in this paper included the neural structures of the barn owl involved in the localization of the azimuthal position of a target. Each structure in the model was composed of a collection of units, each implemented as a leaky integrator

$$\frac{dU_i}{dt} = x_i(t) - \delta U_i(t) + n(t) \tag{1}$$

where $U_i(t)$ is the output of unit i, δ is a constant that determines the decay of activation, $n(t)$ is a noise term, and $x_i(t)$ is the net input to the unit, evaluated as

$$x_i(t) = \sum_k \omega_{ik} U_k(t) \tag{2}$$

where U_k is the activation of unit k connected to unit i through the weight ω_{ik}, which represents the strength of a synapse between the two units. The output, $U(t)$, of a unit

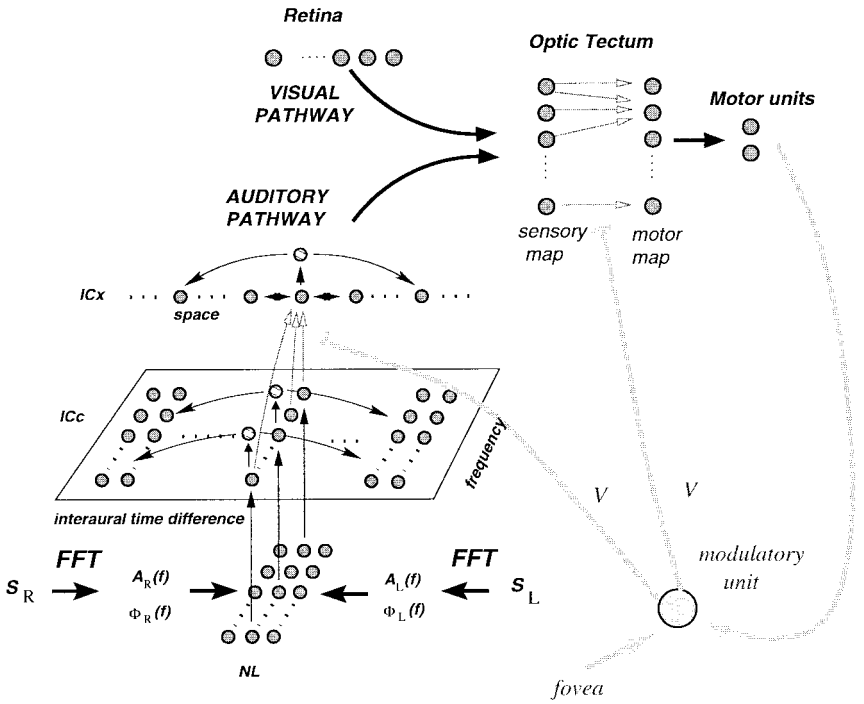

Fig. 2. The model of the barn owl's neural pathways involved in the localization of the azimuth was designed so as to incorporate a large number of physiological and anatomical data. Each area was composed of a collection of units, each implemented as a leaky integrator (see text for details). Solid and striped circles represent excitatory and inhibitory units, respectively. Empty arrows indicate connections with modifiable weights. Inhibitory units at the level of the optic tectum are not shown for clarity.

can be viewed as representing the average firing rate of a collection of cells and its response properties can be considered as representative of a typical cell within such a group. More specifically, in most areas of the model, the net input to the units was evaluated as

$$x_i(t) = \sum_{k \in S_i^{\mathrm{E}}} \omega_{ik}^{\mathrm{E}} U_k^{\mathrm{E}}(t) + \sum_{k \in S_i^{\mathrm{I}}} \omega_{ik}^{\mathrm{I}} U_k^{\mathrm{I}}(t) + \sum_k \omega_{ik} U_k(t) \tag{3}$$

where different contributions are explicitly shown. The first and second terms represent the contributions from excitatory ($\omega_{ik}^{\mathrm{E}} > 0$) and inhibitory ($\omega_{ik}^{\mathrm{I}} < 0$) connections originating from units in the same structure as unit i. The third term represents excitatory inputs from neurons in different structures. S_i^{E} and S_i^{I} are the excitatory and inhibitory neighborhoods of unit i, defined as the sets of units with excitatory connections (excitatory units) and inhibitory connections (inhibitory units) that project to unit i.

Learning occurred in the model by modifying the strengths of selected sets of connections on the basis of sensorimotor experience. According to the proposed learning paradigm, synaptic changes were affected by the activation of a modulatory system modeled after the diffusely projecting subcortical structures such as the monoamingeric and cholinergic systems, common to the brain of many species. The variable connection weights of plastic synapses were initially set to random values and then changed according to a modified version of Hebbian learning [52] inspired by recent findings on synaptic plasticity [53]

$$\frac{d\omega_{ik}}{dt} = \Phi_L(\epsilon_1 U_i U_k + \epsilon_2 V) \tag{4}$$

where V is the activation of the modulatory system (described later in this section) and $\Phi_L(x)$ is a linear piece-wise function characterized by two thresholds θ_D and θ_P (see Fig. 3)

$$\Phi(x) = \begin{cases} 0, & \text{if } x < \theta_D \\ -k_1(x - \theta_D), & \text{if } x \in [\theta_D, \theta') \\ +k_2(x - \theta_P), & \text{if } x \in [\theta', \theta_P) \\ +k_3(x - \theta_P), & \text{if } x \geq \theta_P \end{cases} \tag{5}$$

where $\theta' = (k_2\theta_P - k_1\theta_D)/(k_1 + k_2)$, and k_1, k_2, and k_3 are positive real numbers. It follows from (5), that when the argument of Φ_L is in between the two thresholds the function has a negative value, thus inducing depression of synaptic strengths. Above θ_P it assumes positive values, thereby potentiating the connection. The thresholds were selected so that potentiation occurred only for connections between units whose activity was highly correlated when the activation of the modulatory system was also high. This happened after a successful motor action that brought the stimulus into the fovea, the center of the visual field. By contrast, after a movement that did not lead to localization of the target, connections between highly correlated units tended to be depressed. For each unit, the patterns of weights were periodically normalized. The two terms of the argument of Φ_L have different functional implications: the first term, $\epsilon_1 U_i U_k$, reflects a *local* factor that may be different for different connections; the second term, $\epsilon_2 V$ is a *global* factor shared by all plastic synapses. While the local Hebbian term is proportional to the role played by specific sets of connections in the performed motor behavior, the global term is a reinforcement signal that depends on the behavioral outcome. Both factors are needed for selecting the correct pattern of connection strengths and their relative

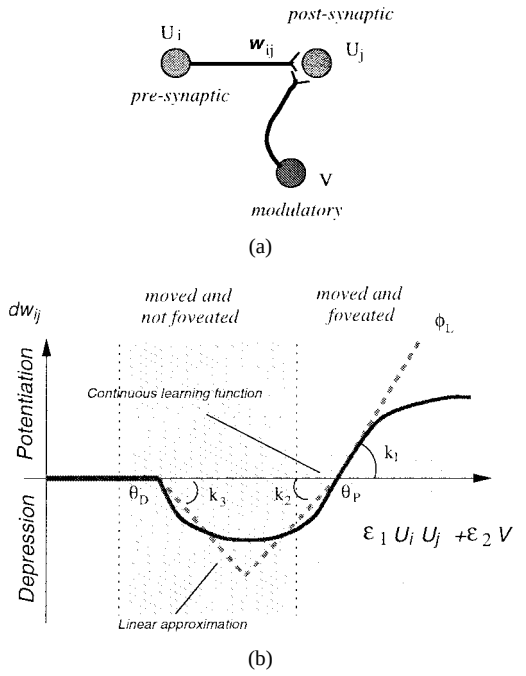

Fig. 3. The learning rule used for changing the strengths of the connections on the basis of sensorimotor experience. (a) The changes in the connection weight w_{ij} between pre-synaptic unit U_i and post-synaptic unit U_j, depend on the activation of the two units and on the activation of the modulatory unit V. (b) A linear approximation, Φ_L, (dashed line) of a biphasic function recently proposed for explaining synaptic plasticity [53] (continuous line), was applied to the sum of the activation of the modulatory term and the correlation of pre- and post-synaptic elements. Due to the learning rule adopted, only those synapses that were active during successful saccades (those which brought the stimulus on the fovea) were strengthened; all others underwent depression.

contribution is set by the values of the parameters ϵ_1 and ϵ_2. Whenever an auditory or visual stimulus is present, the activation of the input units propagates through the network so as to trigger an orienting response. Before the exposure to sensorimotor experience, when the connections have random synaptic strengths, the direction of gaze is in large part determined by the noise superimposed on the activation of the units [see (1)]. Following each movement, connections between highly correlated units (i.e., those connections which gave a significant contribution to the selection of the motor action), are strengthened or weakened depending on whether a foveation event occurred or not, so as to increase or decrease the likelihood of repeating the same action in similar future situations. The influence of noise in unit activation on the selection of movements decreases as the patterns of connectivity become more specific.

In the remaining part of this section, we describe in detail each of the modeled structures and how they relate to the corresponding areas in the barn owl. Structures in the model are indicated by italic characters using the names that refer to the corresponding biological structures.

A. Nucleus Laminaris

As illustrated in Fig. 2, the modeled auditory pathway starts with the nucleus laminaris (NL), which is the first station in the ITD pathway of the barn owl where the signals from the two ears are brought together [36], [54]. The reason for this choice was that the activation of NL neurons can be accurately predicted on the basis of the spectral components of the two input signals. It has been observed that NL neurons in the barn owl are most active at a preferred frequency and their activation is a periodic function of the input ITD [54]. In addition, it has recently been observed that the activity of NL neurons is modulated by the intensity of the binaural stimulation [55]. As in the barn owl, each NL unit was characterized by a preferred frequency, $\overline{f}$, and a preferred input ITD, $\overline{T}$, for which the response of the unit was maximal. For binaural stimulation, when two signals $s_L(t)$ and $s_R(t)$ with Fourier transforms $A_L(f)e^{j\phi_L(f)}$ and $A_R(f)e^{j\phi_R(f)}$ were applied as inputs, the activation $U^{\mathrm{NL}}_{\overline{T},\overline{f}}$ of an NL unit with characteristic parameters $\overline{T}$, $\overline{f}$ was evaluated as

$$U^{\mathrm{NL}}_{\overline{T},\overline{f}} = \mathcal{F}(A_L(\overline{f})A_R(\overline{f}))[\cos(\phi_{LR}(\overline{f}) - 2\pi\overline{f}\overline{T}) + 1]G_{\overline{f}\sigma}(f) \tag{6}$$

where $\mathcal{F}(x)$ is a monotonic function that controls the change in firing rate for different amplitudes of the input signals, $\phi_{LR}(\overline{f}) = \phi_L(\overline{f})$ is the difference of phase between the left and right input signals at frequency $\overline{f}$, and $G_{\overline{f}\sigma}(f)$ is a Gaussian function with mean $\overline{f}$ and variance σ.

Following the physiological data from the barn owl, the NL was modeled as a bidimensional array in which unit sensitivity varied systematically with respect to frequency along one axis and interaural time delays along the other. Within the map, the unit at location (i, j) was characterized by a preferred mean interaural delay $\overline{T}_j$ and by a preferred frequency $\overline{f}_i$

The activation of three units in the NL, as well as the global patterns of activation in the NL map for two auditory targets are shown in Fig. 4(a) and (b), respectively. As illustrated by the figure, the patterns of activation are characterized by a vertical array centered on the column composed of units with preferred ITD equal to the input ITD value. The periodic peaks of activation that change with the frequency of the lamina are the result of the ambiguity in determining the difference of phase of two time-delayed sinusoidal signals.

B. Central Nucleus of the Inferior Colliculus

Based on the known anatomy of the barn owl, the central nucleus of the inferior colliculus (ICc) was modeled as a bidimensional map containing equal numbers of excitatory and inhibitory units. As in the NL, unit layout was such that the sensitivity with respect to ITD and frequency changed systematically along orthogonal directions, so that at each frequency, an array of units (the frequency lamina) with different preferred ITD values is present. As shown in Fig. 2, excitatory units of the ICc received topographically organized projections from the NL. Excitatory units also projected to surrounding units in the ICc and to excitatory units in the ICx, and received connections from inhibitory units in more distant regions of the ICc map. The net input to unit u_{ij} located in position (i, j) in the ICc map was given by (3). For an excitatory unit, the local excitatory and inhibitory

neighborhood in (3) is given by

$$S^{\mathrm{E}_i} = \{u_{kl}\colon \|k-i\| \le d^{\mathrm{E}}\}$$
$$S^{\mathrm{I}_i} = \{u_{kl}\colon d_a^{\mathrm{I}} \le \|k-i\| \le d_b^{\mathrm{I}}\}. \quad (7)$$

In practice, an excitatory unit u_{ij} received external input from the unit located in position (i,j) in the NL map; it received excitatory connections with connection strength β_{E} from ICc excitatory units which were less than d^{E} units distant on the same frequency lamina; and finally, it received inhibitory connections with strength γ from ICc inhibitory units located at a distance between d_a^{I} and d_b^{I} in the same frequency lamina. Inhibitory units received excitatory connections with strength β_I from excitatory units in S^{E_i}. The topographically organized layout of connections from the NL gave rise to systematic changes in the characteristics of ICc units. In agreement with what has been observed in the barn owl [56], the preferred ITD and frequency of ICc units changed along orthogonal axes. The layout of ICc units implies that each array of units perpendicular to the frequency axis, has an array-specific ITD, representing the value of ITD that activates all the units of the array at the same relative response level.

Fig. 4(c) illustrates the sensitivities of three ICc units to different values of ITD. In accord with what occurs in the ICc of the barn owl [38], unit activation was characterized by a narrow frequency range and showed a periodicity with respect to ITD, with the period determined by the neuron's preferred frequency. Two typical maps of activation in the ICc for different auditory targets are shown in Fig. 4(d). The maps are similar to the those in the NL, but due to the influence of inhibitory connections the selectivity of ICc units is more refined.

C. External Nucleus of the Inferior Colliculus

The external nucleus of the inferior colliculus (ICx), is the first site in the ascending pathway to the tectum where information is integrated across multiple frequency channels to create an auditory representation of space. Given that localization of the azimuth only was considered, the ICx was modeled as a one-dimensional array of excitatory and inhibitory units. As illustrated in Fig. 5, projections from the ICc were topographically organized along the ITD axis. Each ICx unit received connections from ICc units in all the frequency laminae, but only from a limited range of preferred ITD's. The probability of a connection between two units decayed with a Gaussian profile of the distance between the ICx unit and the center of the projection area. A spread σ_{ICx} was used in the profile of connection probability. This pattern of connectivity, which provided a rough initial registration between the ICc and ICx, is in accord with the results of anatomical studies in the barn owl [41], [57] as well as the observation that developmental events independent of sensorimotor experience are sufficient to establish a neural connectivity that support rudimentary auditory localization [57]. A local pattern of excitatory and inhibitory connections similar to the ICc was also present in the ICx. This is consistent with data showing that the local connectivity with inhibitory cells has a crucial role in shaping the receptive fields of ICx neurons [58].

Fig. 4(e) and (f), illustrate the response of two ICx units as the ITD between the two input signals was changed systematically. The data refer to a system which had already undergone sensorimotor experience, and the connections between the ICc and ICx had adjusted correspondingly. As a result of the pattern of connectivity, each ICx unit responded maximally to a specific value of ITD, that is, to sound sources located in a specific position of space. In contrast with the responses of units in the NL and in the ICc, units in the ICx did not show periodicity with respect to ITD when stimulated with broad spectrum noise, in agreement with data from the barn owl [59]. As in the barn owl [60], the preferred ITD of ICx units varied systematically with the position of the unit within the map, so as to give rise to a representation of auditory space.

D. Optic Tectum

The OT was modeled as two unidimensional arrays of units: a sensory map composed of bimodal units that were activated by both visual and auditory stimuli, and a motor map whose units projected to the motor system. Both arrays contained excitatory and inhibitory units with a local pattern of connectivity similar to those in the ICc and ICx. OT sensory neurons received visual input directly from the retinal map by means of a set of topographically organized connections (adjacent receptors of the retina are connected to adjacent areas of the OT). In addition, OT sensory units received topographically organized connections from ICx excitatory units. Whereas the visual RF's of OT sensory units were determined by fixed connections from the retina, the auditory RF's could change location depending on plastic changes in the connections from the ICc to the ICx. The mth excitatory unit in the OT sensory map received external input from units in the same position in the ICx and in the retina. It projected with connection strength λ_{jm} to the jth excitatory unit in the motor map. As in the case of the connections between the ICc and the ICx, an initial coarse topographical organization was also present in the connectivity between the sensory and motor maps in the OT. The strengths, λ_{jm}, of the connections were refined during sensorimotor experience. The probability of anatomical connection between units in the sensory and motor maps in the OT decayed with a Gaussian profile of the distance between the motor unit and the center of the projection area. A spread of projection σ_{OT} was used.

E. Motor Output

In order to determine the direction of gaze for a given pattern of activation in the OT, a simplified motor system was implemented. Through a set of fixed connections, OT units in the motor map projected to two motoneurons, which controlled movements to the left and right. The activation of the motoneurons was given by a weighted average of the activation of OT motor units

$$M_k = \sum_j \mu_{kj} O_j \qquad k = 0, 1 \quad (8)$$

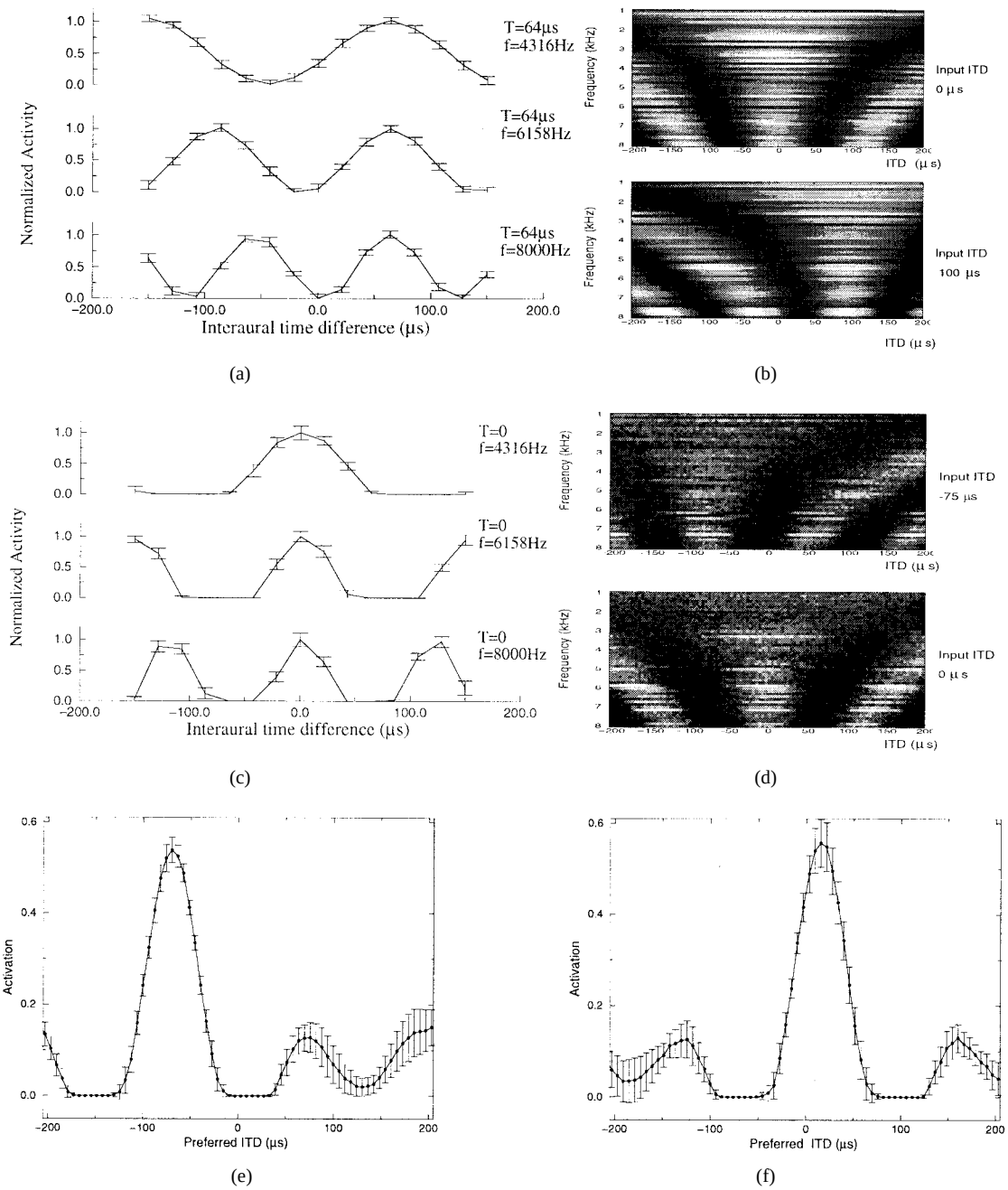

Fig. 4. Responses of units in different areas of the model. Top Row: Characterization of the modeled NL: (a) ITD tuning function of three units with different $\overline{f}$. (b) Two patterns of activation in the NL [(*Top*) ITD $= 0$ μs; (Bottom) ITD $= +100$ μs]: units are aligned in frequency laminae on the y axis, and according to their ITD sensitivity along the x axis. Middle Row: Characterization of the modeled ICc: (a) ITD tuning function of three units in different frequency laminae. (b) Two patterns of activation in the ICc [(Top) ITD $= -75$ μs; (Bottom) ITD $= 0$ μs]. Units are aligned in frequency laminae on the y axis, and according to their ITD sensitivity along the x axis. Bottom Row: Patterns of activation of the modeled ICx when binaural signals with ITD equal to (e) -70 μs and (f) 15 μs are applied as inputs. The graphs show the mean and standard deviation of unit activity evaluated over 10 repetitions.

where O_j is the activation of the jth unit in the motor map of OT and μ_{kj} is the connection strength between this unit and the motoneuron k. To establish a linear relationship between the direction of gaze and the activation of the motor map in OT, the connections strengths μ_{kj} were set to

$$\mu_{kj} = (-1)^k \left(1 - \frac{2j}{N_o}\right) \qquad j = 1, \cdots, N_o; \quad k = 0, 1 \tag{9}$$

In this way, the activation of the first motorneuron increased as the peak of activation moved toward the extreme left of the motor map in the OT. The situation was mirror-symmetric for the second motoneuron and the right side of the map.

The position Φ_h assumed by the system was evaluated through a push-pull relationship, as a function of the activation of the two motoneurons

$$\Phi_h = \frac{\Phi_m}{2}(M_o - M_1) \tag{10}$$

where Φ_m is the maximum movement allowed. By means of the connections μ_{kj}, each unit in the OT motor map triggered

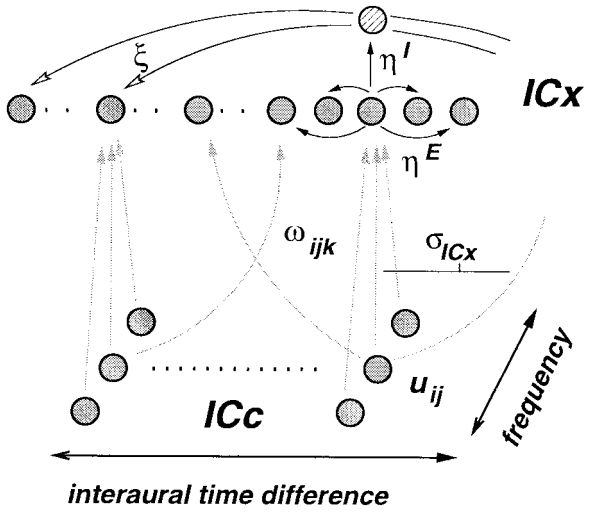

Fig. 5. Connections between the ICc and the ICx and among the units of the ICx. Excitatory units (filled circles) in the ICx received excitatory afferents from units in the ICc and from adjacent units in the ICx. They also received inhibitory afferents from inhibitory units (striped circles) in the ICx located in other regions of the map. They project to neighboring units as well as to the OT (not shown in the figure). Solid arrows indicate excitatory connections, open arrows inhibitory ones. Solid (striped) circles represent excitatory (inhibitory) units.

a shift of gaze by an amount which was proportional to the position of the unit in the map.

F. Modulatory System

In accord with the results of physiological studies on the barn owl [61], [46], experience-dependent changes in the strength of connections occurred both in the projections from the ICc to the ICx and in the projections between sensory and motor maps in the OT. In the learning scheme proposed here, synaptic modifications were mediated by the activation of a modulatory system, which was triggered by the occurrence of visual and motor events. This learning scheme is based on the observation that in the brain of many species relatively small groups of neurons, such as monoaminergic and cholinergic nuclei, project diffusely to large areas of the brain where they modulate neural activity. While little is known about the anatomical and physiological characteristics of monoaminergic and cholinergic systems in the barn owl, the colliculi receive abundant innervation from these systems in most species studied [62], [63]. The modeled modulatory system functionally replicated the hypothesized role of these diffuse-projecting neuromodulatory centers. In view of the complexity of these systems and their interactions, the present model did not attempt to replicate in detail any of their individual properties, but simply represented their overall effect of modulating synaptic plasticity. For simplicity, the modulatory system consisted of a single unit, which received afferents from both the central region of the retina (the fovea) and the motoneurons. Due to the long time constant of units in the motor system, the modulatory system received input throughout the duration of the orienting response and the initial phase of the foveation event. The time constant of the modulatory unit was considerably smaller, such that its level of activation increased nonlinearly if the response to motor events and foveation overlapped in time. In this way, the modulatory unit was moderately active when a stimulus was in the center of the visual field or when a movement was executed, and was particularly active when the two events occurred shortly one after the other. As illustrated in Fig. 3(b), this differential activation of the modulatory unit led to the strengthening or weakening of connections in the model depending on the accuracy of orienting responses.

III. Experimental Results

A preliminary version of the model was analyzed in a series of off-line computer simulations [48]. These simulations revealed that the model can account for the development of a spatial registration between auditory and visual maps in the OT of the barn owl during normal visual experience, after the retinal image was shifted through prismatic goggles, and after the reestablishment of normal visual input. The results of these simulations were in agreement with much of the physiological and behavioral data described in the literature, and also illustrated the robustness of the model with respect to noise and its stability over a wide range of parameters.

In the present study, we analyze the performance of the model when actually used for controlling the orienting behavior of a robotic system in the presence of real visual and auditory targets. The robotic system and the environment used for the experiments are illustrated in Fig. 6. A robotic head (Helpmate Robotics, Danbury, CT) was equipped with a black and white camera and two microphones. As shown in Fig. 6, the camera was mounted at the center of the pan axis of the head, and the two microphones were located at the opposite sides of the camera, at a distance of approximately 30 cm apart. Visual and auditory targets were generated by activating one of 15 lights and loudspeakers located on a circular frame directly in front of the robot. Auditory stimuli consisted of a burst of pseudo-white noise in the frequency range 1–9 Khz. The neural model was implemented on a Unix workstation interfaced to the robot via a VME system, and the motor commands of the model were used to control the pan position of the robotic head. The selection of the target was also controlled by the host workstation via a digital I/O board. Visual and auditory data were processed in real-time by dedicated boards on the VME. The sampled image was thresholded on a Datacube MV200 (Danvers, MA) and the pixel values summed up along the vertical axis of the image, so as to produce a vector which was used as the input activation of the retina. The two auditory channels were simultaneously sampled and their FFT's estimated continuously on a dedicated multi-channel DSP.

In all the experiments described in this section, the experimental paradigm consisted of three sequential steps: first, the system was positioned so as to aim in a randomly selected direction. A visual or an audiovisual target was then presented at one of the 15 available locations, and as a result the head moved according to the activity determined within the neural model. After the execution of the movement, the stimuli were removed and the accuracy of localization performance was

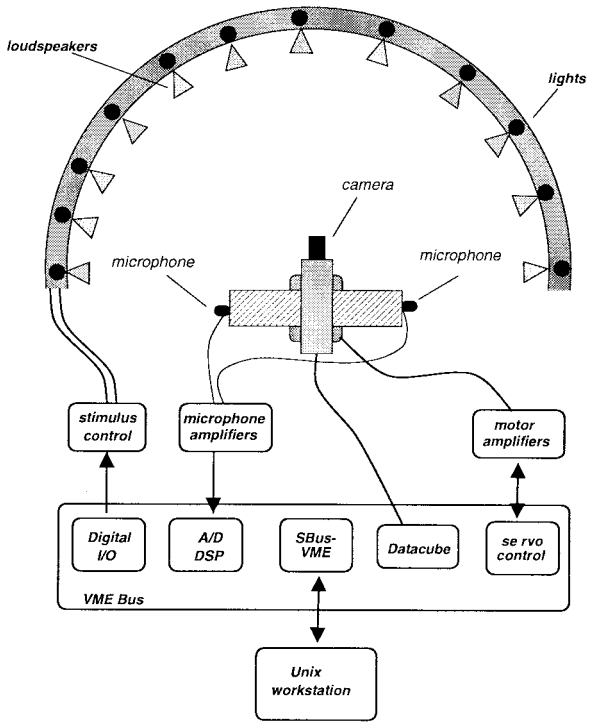

Fig. 6. System architecture controlled by the neural model. The camera was mounted at the center of the pan axis of a TRC robotic head. Visual signals were acquired and processed by a Datacube MV200 board. Real-time processing consisted in the thresholding of the image and compression along the azimuthal axis. Auditory signals were acquired by two microphones located at the opposite sides of the camera, and they were digitized by synchronized A/D channels. FFT's of both channels were evaluated in real-time on a DSP board. The system was positioned at the center of a circular array which included 15 lights and loudspeakers. Selected targets were activated via a digital I/O board on the VME bus.

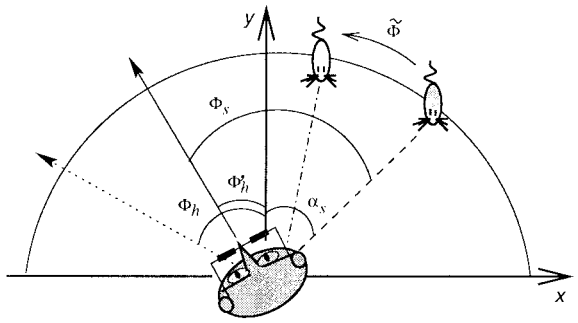

Fig. 7. The experimental procedure consisted of randomly selecting the initial direction of gaze Φ_h (dotted line) and the position of the target α_s. Φ_h' indicates the direction of gaze assumed by the system after the first orienting movement. The foveation error was defined as the distance between the center of the retina and the center of the target projection on the retina. In the absence of manipulations of the visual input, the foveation error is equal to the orientation error, that is the angle Φ_s between the position assumed by the system and the location of the target. In the case of a translation of the visual input by an angle $\bar{\Phi}$ (see text), the foveation error is equal to the angle $\Phi_s - \bar{\Phi}$ between the position assumed by the system and the apparent location of the target.

TABLE I
RANGES OF VALUES OF THE MODEL PARAMETERS USED IN THE EXPERIMENTS

	parameter	value
Model anatomy	σ	400 Hz
	δ	0.1 - 0.7
	n	0.1
	freq. range	1 - 9 Khz
	ITD range	-800 - 800μs
	d^E	2 - 3
	d_a^I	5 - 6
	d_b^I	25 - 30
	Φ_m	180^o
Synaptic connections	σ_{ICx}	10 - 30
	σ_{OT}	10 - 30
	γ, ξ	0.006 - 0.33
	β^i, η^i	0.001 - 0.05
	β^e, η^e	0.1 - 0.5
	λ_k	1.0
Synaptic plasticity	ϵ_1	0.1 - 0.4
	ϵ_2	0.6 - 0.9
	k_1	0.01 - 0.03
	k_2	-0.001, -0.005
	k_3	-0.001, -0.02
	θ_D	0.2 - 0.4
	θ_P	0.6 - 0.8

measured. Periodically, in order to evaluate quantitatively the accuracy of the system, visual and auditory targets at several fixed distances from the current direction of gaze were presented and foveation errors (see Fig. 7) were measured. The results described in this paper refer to a model composed of 50×300 units in both NL and ICc, and 50 units in all the other maps. The values of the parameters of the model are shown in Table I.

A. Development of Orienting Behavior

The first series of experiments focused on the development of orienting behavior in the presence of normal sensorimotor conditions. Normal conditions refer to the situation in which no systematic manipulation of sensorimotor characteristics was performed, in contrast to the experiments described later. The goal of these experiments was to discover the sensorimotor transformations that lead to successful localization of the target, given the relative structural arrangements of the system components and their functional characteristics. As previously described, the adopted learning scheme was such that connections both at the level of the ICx and OT changed their strengths as a result of behavioral performance.

Before the exposure to sensorimotor experience, the orientation behavior of the system was poor, due to the initial random strengths of connections in the model. The initial performance of the system was dependent on the spread of projections in the ICx and OT and on the level of noise superimposed onto unit activation. Given the initial broad sensory tuning of ICx and OT units, the level of noise in the activation of the cells had an important role in determining the final position assumed by the system, thus giving rise to high variability in the final position. By means of learning, the performance of the system improved with sensorimotor experience, and the mean and standard deviation of the foveation error both decreased. These reductions were a consequence of a decreased influence of noise on behavior due to an increased specificity of unit activation.

In the experiment reported in Fig. 8 the initial magnitude of the foveation error was $20.14° \pm 28.41°$ for visual targets and

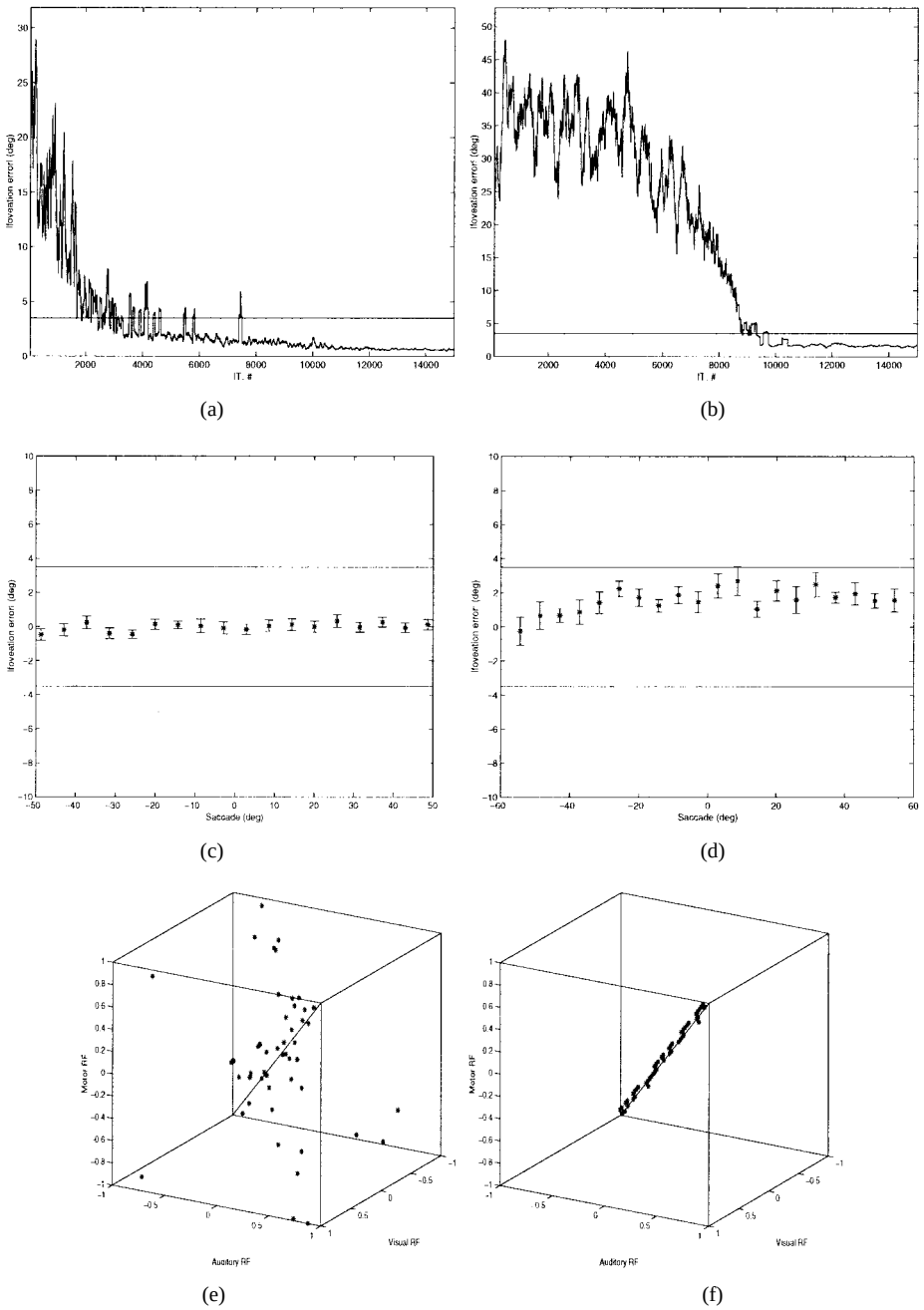

Fig. 8. Improvement of system performance with sensorimotor experience. (Top row) Improvement in the accuracy of orienting behavior toward visual (a) and auditory (b) targets with learning. The plot is a running average over 50 movements. The horizontal lines in the graphs indicate the dimension of the fovea, which consisted of three receptors corresponding to a spatial extension of 7°. (Middle row) Foveation errors (y axis) after the presentation of 15 000 targets for stimuli in different spatial locations (x axis): visual targets (c) and auditory targets (d). (Bottom row) Relative alignment of the auditory, visual and motor receptive fields for the units of the OT, before (e) and after (f) sensorimotor experience. The main diagonal $x = y = z$ on which the RF's align is also shown.

39.29° $\pm$ 32.69° for auditory targets. Fig. 8(a) and (b) shows the mean change in the absolute foveation error at different times during the presentation of 15 000 visual [Fig. 8(a)] and audiovisual [Fig. 8(b)] targets, the equivalent of a few hours of training. Fig. 8(c) and (d) illustrates the final mean foveation error in the system for visual and auditory targets in different spatial positions relative to the direction of gaze. Overall the magnitude of the foveation error dropped to 0.59°$\pm$ 0.38° for visual localization and to 1.54°$\pm$ 1.01° for auditory localization. During the localization of visual stimuli, learning occurred mainly at the level of the OT, while both the OT and ICx were affected for movements in response to audiovisual targets. Following the conventions commonly adopted in neurophysiology, we defined the center of a visual (auditory) RF as the position of a visual (auditory) stimulus position that gives rise to the maximum value of activation of the unit. The center of a motor RF was defined as the mean spatial location assumed by the system when the unit was activated, as in microstimulation experiments [40]. Fig. 8(e) and (f) shows the alignment of auditory, visual and motor RF's for OT units, before and after training, respectively. For each unit, a dot is plotted at a position defined by the

centers of its RF. When the RF's are perfectly in register, the points lie on the principal diagonal (the line $x = y = z$) and the distance of the RF's from this line can be used as a measure of the alignment. The relative alignment between RF's improved drastically with learning, with the distance dropping from 24.77°± 27.24° to 1.15°± 0.95°.

B. Adaptation to Altered Sensory Conditions

In order to test the robustness of the system with respect to altered sensory conditions, we replicated some well-known experiments of sensory manipulation in the barn owl. A striking example of adaptation of orienting behavior is given by experiments in which the visual input is chronically translated by inserting prismatic goggles over the eyes of the barn owl. It has been found that prolonged exposure in early life to a translated visual field causes the animal to recalibrate the orienting behavior toward auditory targets. Instead of aiming directly toward the sound source, barn owls learn to direct their gaze laterally by an extent equal to the shift introduced by the prisms [64], [43], so that after execution of the motor action targets project onto the fovea. Furthermore, if removal of the sensory manipulations occurs sufficiently early in life, a barn owl is usually able to recover normal behavior.

In this section, we describe the results of two sets of sensory manipulation experiments. In the first paradigm, a translation of the visual field was present from the start of sensorimotor experience, thus replicating the insertion of the goggles when the owl first opens its eyes. In the second paradigm, the shift of the visual field was introduced after the system had become well adapted to normal sensorimotor experience. This second set of experiments replicated the insertion of prismatic goggles over the eyes of older barn owls, and were useful in determining the ability of the system to recover from sudden changes in the sensory characteristics. In both cases, the translation of the sampled image was achieved by shifting it directly on the video acquisition board in the VME system.

In an example of development of orienting behavior in the presence of chronic translation of the visual field, the image was translated by 20° to the right. The system had no difficulty in developing accurate localization, so that, with learning, the magnitude of the foveation error decreased from $29.05° \pm 27.89°$ to $-0.61° \pm 0.38°$ for visual targets and from $30.92° \pm 23.17°$ to $2.28° \pm 1.05°$ for auditory targets. After the presentation of 15 000 targets, the foveation error was less then the size of the fovea for both visual and auditory targets located at any distance away from to the current direction of gaze. As in the case of normal sensorimotor experience, the improvement of orienting behavior originated from the increased accuracy in the alignment between sensory and motor maps in the OT. In this case, since accurate localization implies that the system aims at the side of the target by an amount that compensates for the presence of the goggles, visual and auditory RF's were in close alignment and were systematically shifted with respect to the motor RF's. After learning, the distance of the RF's from the line $x = y = z+$ 20° dropped from $30.31° \pm 24.60°$ to $1.4° \pm 0.73°$.

Fig. 9 illustrates the ability of the model to recover from a sudden change in visual inputs. The system had been previously exposed to normal sensorimotor experience (performance illustrated in Fig. 8) when the visual field was translated by 20° to the right. As illustrated by Fig. 9(a), the localization of visual targets remained accurate after the shift was introduced. This is similar to what occurs in the barn owl, and is a consequence of the fact that the alignment between visual and motor maps in the OT does not need to be changed, since the magnitude of movements leading to the localization of visual targets is not affected by the goggles. On the contrary, the audiomotor coordination needs to be readjusted in the presence of a translated visual field [see Fig. 9(b)], as auditory inputs need to trigger different motor actions. The final performance of the system is shown in Fig. 9(c) and (d). Again, the absolute foveation error is less than the size of the fovea for visual and auditory stimuli in different spatial positions ($0.65° \pm 0.45°$ for visual targets and $2.15° \pm 1.02°$ for auditory targets). Fig. 9(e) and (f) illustrates that the recovery of good orientation accuracy was again a consequence of reacquired alignment between the visual and auditory maps in the OT. Immediately after the introduction of the visual shift, although the RF's remained aligned along a straight line, they were shifted away from the main diagonal ($x = y = z$) by an amount equal to visual displacement [see Fig. 9(e)]. With sensorimotor experience, the RF's become aligned on the line $x = y = z+$ 20° [Fig. 9(f)], so that the final distance of the RF's from this line is $2.12° \pm 3.22°$.

C. Adaptation to Altered Motor Conditions

To analyze the capability of the system to adapt to changes in the motor characteristics, experiments were conducted in which the motor behavior of the model was systematically altered. Manipulations of the motor outputs were implemented by directly modifying the motor commands sent by the model to the robot. In this section, we describe the performance of the system in the presence of a nonlinear motor transformation, in which the direction of gaze Φ' was evaluated as

$$\Phi' = \mathrm{sgn}(\Phi)\Phi_M\left(\frac{\Phi}{\Phi_M}\right)^2$$

where Φ is the output of the model given by (10). This manipulation, which is similar to a nonlinear change in the gain of the motors, introduces a modification in the way the pattern of activation in the OT affects motor behavior. This is equivalent to an anisotropic displacement of the OT motor map and it represents a condition which can be approximated by, for example, damaging the muscles of the neck in the barn owl. As in the case of alteration of the sensory inputs, we considered the introduction of motor manipulations at the onset of sensorimotor experience and also in a well-trained system.

When a motor manipulation was introduced in the early phases of sensorimotor experience, the system was able to learn the sensorimotor transformations so as to produce accurate orienting behavior. After the presentation of 15 000 stimuli, the mean magnitude of the foveation error dropped to 1.76° ± 1.29° for visual targets, and to 2.2°± 1.4° for auditory targets.

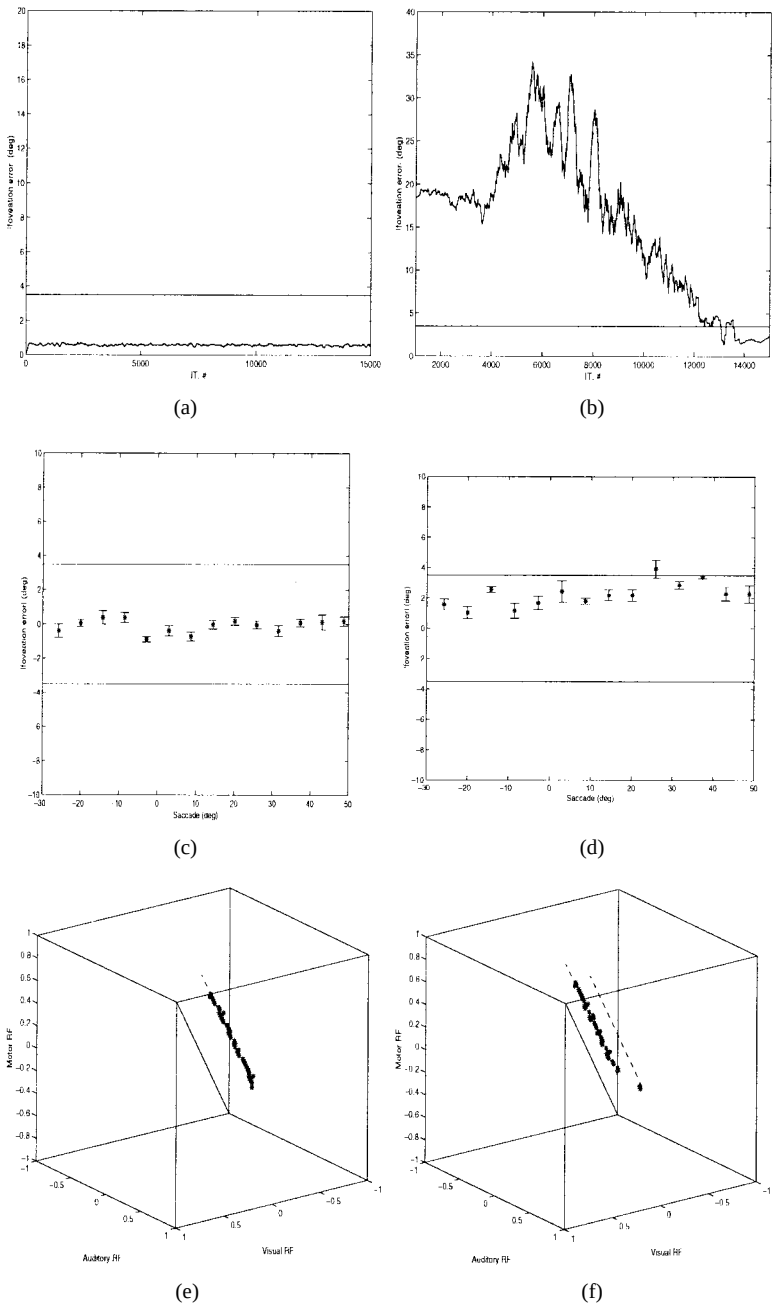

Fig. 9. System performance in the presence of a sudden change of visual characteristics. A system previously trained with normal sensorimotor experience was exposed to a systematic translation of the visual field by 20° to the right. (Top row) Improvement in the accuracy of orienting behavior toward visual (a) and auditory (b) targets with learning. (Middle row) Foveation errors after the presentation of 15 000 targets for stimuli in different spatial locations: visual targets (c) and auditory targets (d). (Bottom row) Relative alignment of the auditory, visual and motor receptive fields for the units of the OT, before (e) and after (f) the new sensorimotor experience.

Fig. 10 shows the ability of the system to recover from a sudden change in motor characteristics, such as may occur due to a motor malfunction. At the beginning, immediately after the change in the motor characteristics, errors were present in the localization of both visual (9.88°$\pm$ 3.95°) and auditory targets (10.09°$\pm$ 4.52°). After the presentation of 15,000 stimuli the orientation error was reduced to 1.04°$\pm$ 0.83° and 1.83° $\pm$ 1.31° for visual and auditory targets, respectively. As in the case of sensory manipulation, the recovery of orientation accuracy was a consequence of the reacquired alignment of the receptive fields for the units in OT. The nonlinear motor transformation introduced in this experiment is reflected by the RF alignment function shown in Fig. 10(e) (the mean RF distance with respect to the line $x = y = z$ was 7.85°$\pm$ 3.38°). Learning is able to realign the maps of space as reflected by the linear correspondence of RF's in Fig. 10 (f), so that the final distance of RF's with respect to $x = y = z$ was 1.56°$\pm$1.14°.

IV. Conclusion

Robustness is a crucial issue in the design of autonomous systems. Environmental conditions change continuously due to a number of unpredictable factors, as do the characteristics

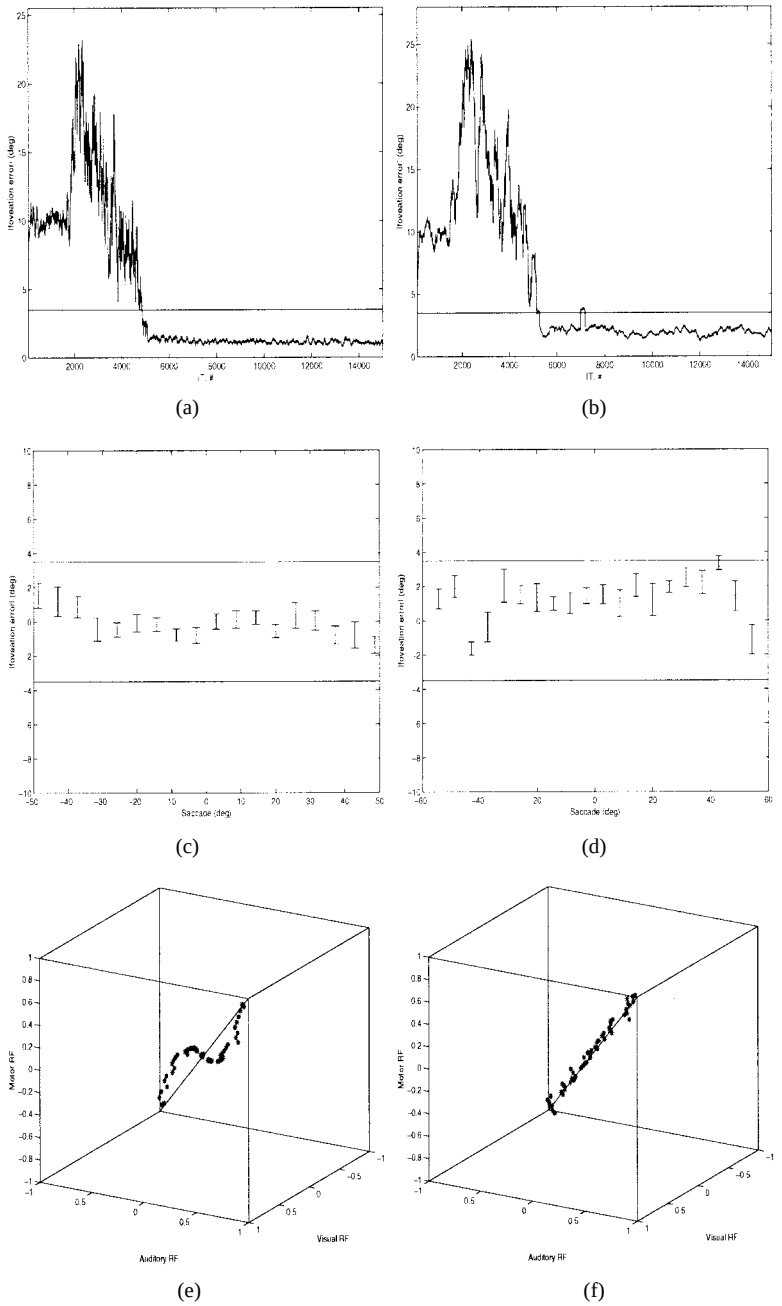

Fig. 10. System performance in the presence of a sudden change of motor characteristics. (Top row) Improvement in the accuracy of orienting behavior toward visual (a) and auditory (b) targets with learning. (Middle row) Foveation errors after the presentation of 15 000 targets for stimuli in different spatial locations: visual targets (c) and auditory targets (d). (Bottom row) Relative alignment of the auditory, visual and motor receptive fields for the units of the OT, before (e) and after (f) the new sensorimotor experience.

of sensors and motors. In order to maintain good performance in the presence of such changes, autonomous systems need to continuously accommodate their behavior to the current conditions. Biological systems provide clear examples of such adaptive capabilities. Individuals of virtually every animal species show significant variations in their phenotypic appearance and their bodies undergo large changes during their lifetime. Nevertheless, their brains are constantly able to tune motor output so as to ensure proper behavior.

Understanding the principles underlying learning and adaptation is one of the major goals of the biological sciences. It is clear that changes in behavior originate from changes at the cellular level, and that different levels of explanation are required in order to have a complete picture of how learning occurs. The case of spatial localization in the barn owl is one of the few examples described in the literature in which quantitative changes in a motor output (the adjustment of orienting behavior) have been systematically linked in detail to neural phenomena (the plastic alignment between sensory and motor maps in the OT). Anatomical and physiological studies have extensively characterized the structures in the brain of the barn owl involved in the production of orienting behavior, and provide serious constraints on the underlying mechanisms of learning. The hypothesis proposed here that map registration

occurs through a mechanism of value-dependent learning does not require the existence of any unknown anatomical pathways or structures nor does it imply biologically unrealistic computations. In addition, a large body of evidence supports the idea that synaptic plasticity is mediated by a global signal related to the saliency of sensorimotor events. In many different species neuromodulatory systems have been found that project diffusely to most areas of the brain. These systems, such as the monoaminergic and cholinergic systems in vertebrates are endowed with the appropriate anatomical and physiological properties, and there is evidence that they play a role in long-term plasticity (see references in [48]). The results of this paper, together with close comparisons between behavioral and physiological data from the barn owl and equivalent data obtained from computer simulations are strongly in accord with this proposal.

In the past, researchers in robotics and AI have often looked at biology as a source of inspiration for solving their problems. From the opposite perspective, neuroscientists have recently turned their attention toward the use of robotic systems as a way to quantitatively test and analyze theories that would otherwise remain at a speculative stage. The approach of synthetic neural modeling [5], [6] is based on the coupling of computational models of brain structures with systems interacting in the real world. While computer models have recently gained popularity in the neuroscience community as a way to analyze the operations of complex neuronal ensembles, these models are usually activated with simplified artificial patterns that bear little resemblance to natural stimuli. The use of robotic systems has the advantage of introducing phenotypic and environmental constraints similar to those that brains of animals have to face during development. Consideration of these constraints is particularly important in light of modern brain theories, that emphasize the importance of the environment and sensorimotor experience during neural development.

There is little doubt that comprehension of the fundamental functional principles of the brain will dramatically affect the design of artificial systems operating in the real-world. We believe that the approach of synthetic neural modeling and efforts like the one described in this paper can make a significant contribution toward these goals and, at the same time, by establishing a direct link between the natural and engineering sciences, offer new ideas to workers in robotics and artificial intelligence.

REFERENCES

[1] J. S. Albus, *Brains, Behavior, and Robotics.* Peterborough, NH: BYTE Books, 1981.

[2] C. Mead, *Analog VLSI and Neural Systems.* Reading, MA: Addison-Wesley, 1989.

[3] N. H. Franceschini, "Vision, flies, neurons and robots," in *Proc. IEEE Int. Conf. Robot. Automat.*, 1995, pp. 3165–3170.

[4] M. V. Srinivasan and S. Venkatesh, *From Living Eyes to Seeing Machines.* Oxford, U.K.: Oxford Univ. Press, 1997.

[5] G. M. Edelman, *Neural Darwinism.* New York: Basic Books, 1987.

[6] G. N. Reeke, O. Sporns, and G. M. Edelman, "Synthetic neural modeling: The "Darwin" series of recognition automata," *Proc. IEEE*, vol. 78, pp. 1496–1530, Sept. 1990.

[7] W. T. Miller, R. S. Sutton, and P. J. Werbos, *Neural Networks for Control.* Cambridge, MA: MIT Press, 1990.

[8] V. D. Sánchez and G. Hirzinger, "The state of the art of robot learning control using artificial neural networks: An overview," in *The Robotics Review 2*, O. Khatib, J. J. Craig, and J. Lozano-Perez, Eds. Cambridge, MA: MIT Press, 1992.

[9] G. Sandini, G. Gandolfo, F. Grosso, and M. Tistarelli, "Vision during action," in *Active Perception*, Y. Aloimonos, Ed. Hillsdale, NJ: Erlbaum, 1993, pp. 151–190.

[10] A. L. Abbott, "A survey for selective fixation control for machine vision," *IEEE J. Contr. Syst.*, pp. 25–31, Aug. 1992.

[11] P. J. Burt, "Smart sensing within a pyramid vision machine," *Proc. IEEE*, vol. 76, pp. 1006–1015, Aug. 1988.

[12] C. Colombo, M. Rucci, and P. Dario, "Attentive behavior in an anthropomorphic robot vision system," *J. Robot. Auton. Syst.*, 1994.

[13] R. Bajcsy, "Active perception," *Proc. IEEE*, vol. 76, pp. 996–1005, Aug. 1988.

[14] J. Aloimonos, I. Weiss, and A. Bandyopadhyay, "Active vision," *Int. J. Comput. Vis.*, vol. 1, no. 4, pp. 333–356, 1988.

[15] D. H. Ballard, "Animate vision," *Artif. Intell.*, vol. 48, pp. 57–86, 1991.

[16] I. Sobel, "On calibrating computer controlled cameras for perceiving 3-D scenes," *Artif. Intell.*, vol. 5, pp. 185–198, 1974.

[17] O. D. Faugeras and G. Toscani, "The calibration problem for stereo," in *Proc. IEEE Conf. Comput. Vision Pattern Recog.*, 1986, pp. 15–20.

[18] K. S. Fu, R. C. Gonzalez, and C. S. G. Lee, *Control, Sensing, Vision and Intelligence.* New York: McGraw-Hill, 1987.

[19] R. K. Lenz and R. Y. Tsai, "Techniques for calibration of the scale factor and image center for high accuracy 3D machine vision metrology," *IEEE Trans. Pattern Anal. Machine Intell.*, vol. 10, pp. 713–720, 1988.

[20] Y. C. Shiu and S. Ahmad, "Calibration of wrist-mounted robotic sensors by solving homogeneous transform equations of the form $ax = xb$," *IEEE Trans. Robot. Automat.*, vol. 5, pp. 16–29, Feb. 1989.

[21] B. Espiau, F. Chaumette, and P. Rives, "A new approach to visual servoing in robotics," *IEEE Trans. Robot. Automat.*, vol. 8, pp. 313–326, June 1992.

[22] S. Hutchinson, G. D. Hager, and P. I. Corke, "A tutorial on visual servo control," *IEEE Trans. Robot. Automat.*, vol. 12, pp. 651–670, Oct. 1996.

[23] J. T. Feddema and O. R. Mitchell, "Vision-guided servoing with feature-based trajectory generation," *IEEE Trans. Robot. Automat.*, vol. 5, pp. 691–700, Oct. 1989.

[24] N. P. Papanikolopoulos, B. J. Nelson, and P. K. Khosla, "Six degree-of-freedom hand/eye visual tracking with uncertain parameters," *IEEE Trans. Robot. Automat.*, vol. 11, pp. 725–732, Oct. 1995.

[25] B. H. Yoshimi and P. K. Allen, "Alignment using an uncalibrated camera system," *IEEE Trans. Robot. Automat.*, vol. 11, pp. 516–521, Aug. 1995.

[26] E. Grosso, G. Metta, A. Oddera, and G. Sandini, "Robust visual servoing in 3-D reaching tasks," *IEEE Trans. Robot. Automat.*, vol. 12, pp. 732–741, Oct. 1996.

[27] G. D. Hager, "A modular system for robust positioning using feedback from stereo vision," *IEEE Trans. Robot. Automat.*, vol. 13, pp. 582–595, Aug. 1997.

[28] D. J. Bennet, D. Geiger, and J. M. Hollerbach, "Autonomous robot calibration for hand-eye coordination," *Int. J. Robot. Res.*, vol. 10, no. 5, pp. 550–559, 1991.

[29] S. J. Maybank and O. Faugereas, "A theory of self-calibration of a moving camera," *Int. J. Comput. Vision*, vol. 8, pp. 123–151, 1992.

[30] F. Du and M. Brady, "Self-calibration of the intrinsic paramaters of camera for active vision systems," in *Proc. IEEE Conf. Comput. Vision Pattern Recog.*, 1993.

[31] R. I. Hartley, "Self-calibration from multiple views with a rotating camera," in *Proc. 3rd Euro. Conf. Comput. Vision*, 1994, pp. 471–478.

[32] P. F. McLauchlan and D. W. Murray, "Active camera calibration for a head-eye platform using the variable state-dimension filter," *IEEE Trans. Pattern Anal. Machine Intell.*, vol. 18, no. 1, Jan. 1996.

[33] S. D. Ma, "A self-calibration technique for active vision systems," *IEEE Trans. Robot. Automat.*, vol. 12, pp. 114–120, Feb. 1996.

[34] M. Rucci and R. Bajcsy, "Learning visuo-tactile coordination in robotic systems," in *Proc. IEEE Conf. Robot. Automat.*, 1995, pp. 2678–2683.

[35] M. Konishi, "How the owl tracks its prey," *Amer. Sci.*, vol. 61, pp. 414–424, 1973.

[36] ———, "Listening with two ears," *Sci. Amer.*, vol. 268, no. 4, pp. 34–41, 1993.

[37] B. E. Stein and M. A. Meredith, *The Merging of the Senses.* Cambridge, MA: MIT Press, 1993.

[38] M. Konishi, T. T. Takahashi, H. Wagner, W. E. Sullivan, and C. E. Carr, "Neurophysiological and anatomical substrates of sound localization in the owl," in *Auditory Function: Neurobiological Bases of Hearing*, G. M. Edelman, W. E. Gall, and W. M. Cowan, Eds. New York: Wiley, 1988, pp. 721–744.

[39] M. Konishi, "Centrally synthesized maps of sensory space," *Trends Neurosci.*, vol. 9, pp. 163–168, 1986.

[40] S. du Lac and E. I. Knudsen, "Maps of head movement vector and speed in the optic tectum of the barn owl," *J. Neurophys.*, vol. 63, pp. 131–146, 1990.
[41] E. I. Knudsen, "Subdivision of the inferior colliculus in the barn owl (*tyto alba*)," *J. Comp. Neur.*, vol. 218, pp. 174–186, 1983.
[42] ———, "Experience shapes sound localization and auditory unit properties during development in the barn owl," in *Auditory Function: Neurobiological Bases of Hearing*, G. M. Edelman, W. E. Gall, and W. M. Cowan, Eds. New York: Wiley, 1988, pp. 137–148.
[43] E. I. Knudsen and M. S. Brainard, "Visual instruction of the neural map of auditory space in the developing optic tectum," *Science*, vol. 253, pp. 85–87, 1991.
[44] J. Mogdans and E. I. Knudsen, "Adaptive adjustment of unit tuning to sound localization cues in response to monaural occlusion in developing owl optic tectum," *J. Neurosci.*, vol. 12, pp. 3473–3484, 1992.
[45] E. I. Knudsen and J. Mogdans, "Vision independent adjustment of unit tuning to sound localization cues in response to monaural occlusion in developing owl optic tectum," *J. Neurosci.*, vol. 12, pp. 3485–3493, 1992.
[46] M. S. Brainard and E. I. Knudsen, "Experience-dependent plasticity in the inferior colliculus: A site for visual calibration of the neural representation of auditory space in the barn owl," *J. Neurosci.*, vol. 13, no. 11, pp. 4589–4608, 1993.
[47] J. Mogdans and E. I. Knudsen, "Site of auditory plasticity in the brain stem (vlvp) of the owl revealed by early monaural occlusion," *J. Neurophysiol.*, vol. 12, pp. 2875–2890, 1994.
[48] M. Rucci, G. Tononi, and G. M. Edelman, "Registration of neural maps through value-dependent learning: Modeling the alignment of auditory and visual maps in the barn owl's optic tectum," *J. Neurosci.*, vol. 17, no. 1, pp. 334–352, 1997.
[49] A. G. Barto, R. S. Sutton, and C. W. Anderson, "Neuronlike adaptive elements that can solve difficult learning control problems," *IEEE Trans. Syst., Man, Cybern.*, vol. SMC-13, pp. 834–846, May 1983.
[50] L. P. Kaebling, M. L. Littman, and A. W. Moore, "Reinforcement learning: A survey," *J. Artif. Intell. Res.*, vol. 4, pp. 237–285, 1996.
[51] K. J. Friston, G. Tononi, G. N. Reeke, O. Sporns, and G. M. Edelman, "Value-dependent selection in the brain: Simulation in a synthetic neural model," *Neurosci.*, vol. 59, no. 2, pp. 229–243, 1994.
[52] D. O. Hebb, *The Organization of Behavior*. New York: Wiley, 1949.
[53] A. Artola and W. Singer, "Long-term depression of excitatory synaptic transmission and its relationship to long-term potentiation," *Trends Neurosci.*, vol. 16, no. 11, pp. 480–487, 1993.
[54] C. E. Carr and M. Konishi, "A circuit for detection of interaural time differences in the brain stem of the barn owl," *J. Neurosci.*, vol. 10, no. 10, pp. 3227–3246, 1990.
[55] J. L. Peña, S. Viete, Y. Albeck, and M. Konishi, "Tolerance to sound intensity of binaural coincedence detection in the nucleus laminaris of the owl," *J. Neurosci.*, vol. 16, no. 21, pp. 7046–7054, 1996.
[56] H. Wagner, T. T. Takahashi, and M. Konishi, "Representation of interaural time difference in the central nucleus of the barn owl's inferior colliculus," *J. Neurosci.*, vol. 74, pp. 3105–3116, 1987.
[57] E. I. Knudsen, "Synthesis of a neural map of auditory space in the owl," in *Dynamic Aspects of Neocortical Function*, G. M. Edelman, W. M. Cowan, and W. E. Gall, Eds. New York: Wiley, 1984, pp. 375–396.
[58] I. Fujita and M. Konishi, "The role of gabaergic inhibition in processing of interaural time difference in the owl's auditory system," *J. Neurosci.*, vol. 11, pp. 722–739, 1991.
[59] T. T. Takahashi and M. Konishi, "Selectivity for interaural time difference in the owl's midbrain," *J. Neurosci.*, vol. 6, pp. 3413–3422, 1986.
[60] E. I. Knudsen, M. Konishi, and J. D. Pettigrew, "Receptive fields of auditory neurons in the owl," *Science*, vol. 198, pp. 1278–1280, 1977.
[61] S. du Lac and E. I. Knudsen, "Early visual deprivation results in a degraded motor map in the optic tectum of barn owls," *Proc. Nat. Acad. Sci. USA*, vol. 88, pp. 3426–3430, 1991.
[62] S. B. Edwards, C. L. Ginsburgh, C. K. Henkel, and B. E. Stein, "Sources of subcortical projections to the superior colliculus in the cat," *J. Comp. Neurol.*, vol. 184, pp. 309–330, 1979.
[63] G. C. Thompson, A. M. Thompson, K. M. Garrett, and B. H. Britton, "Serotonin and serotonin receptors in the central auditory system," *Otolaryngology Head Neck Surgery*, vol. 110, no. 1, pp. 93–102, 1994.
[64] E. I. Knudsen and P. F. Knudsen, "Vision calibrates sound localization in developing barn owls," *J. Neurosci.*, vol. 9, pp. 3306–3313, 1989.

Michele Rucci (S'92–M'95) received the laurea degree (summa cum laude) in bioengineering from the University of Florence, Italy, and the Ph.D. degree from the Scuola Superiore S. Anna, Pisa, Italy.

In 1994, before joining The Neurosciences Institute, San Diego, CA, he was a Visiting Researcher with the University of Pennsylvania, Philadelphia. His research interests are in the field of perception and learning both in biological and artificial systems. He has undertaken an interdisciplinary approach which involves the use of mathematical and computational techniques to investigate the basic principles of neural systems and the application of such principles to the development of new algorithms in machine perception. He is particularly interested in the analysis of complete sensorimotor loops and in the use of robotic systems to expose neural models to the nonidealized characteristics of real environments. He is the author of publications in both biological and engineering journals.

Dr. Rucci is a Fellow in Computational Neuroscience at The Neurosciences Institute.

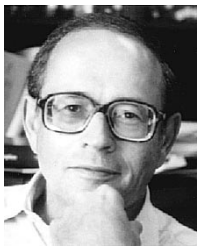

Gerald M. Edelman received the B.S. degree from Ursinus College, Collegeville, PA, the M.D. degree from the University of Pennsylvania, Philadelphia, and the Ph.D. degree from the Rockefeller Institute, New York, NY. He has also received numerous honorary D.Sc. degrees from institutions as diverse as Williams College, the University of Paris, and the University of Cagliari, Sardinia, Italy.

He is the President of Neurosciences Research Foundation and Director of The Neurosciences Institute, San Diego, CA, as well as the Chairman of the Department of Neurobiology, The Scripps Research Institute. He then began research into the mechanisms involved in the regulation of primary cellular processes, particularly the control of cell growth and the development of multicellular organisms. In work focusing on cell–cell interactions, he identified cell adhesion molecules (CAM's), which help guide the fundamental processes by which an animal achieves its shape and form and by which nervous systems are built. At the juncture of these two discoveries lies the basis of his theory of the development and organization of higher brain functions in terms of a process known as "neuronal group selection," described in his book *Neural Darwinism* (1987). He is the author of several books and over 400 research publications.

Dr. Edelman received the Nobel Prize for his early studies of the structure and diversity of antibodies. He is a member of the National Academy of Sciences, the American Philosophical Society, and the Institute de France.

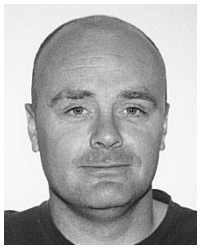

Jonathan Wray was born in Yorkshire, U.K. in 1966. He received the B.Eng. degree in electrical and electronic engineering and the Ph.D. degree in physiology from the University of Newcastle upon Tyne, U.K. His thesis work involved the mathematical analysis of neural networks, the formal comparison of such systems with classical techniques, and the use of networks in nonlinear analysis of single cell biophysics.

He is an Institute Fellow in Theoretical Neurobiology at the Neurosciences Institute, San Diego, CA, were he has developed his interests in systems neuroscience. His current research interests include the neural basis of perception and sensorimotor coordination which he studies using large-scale computer simulations of nervous systems.

Dr. Wray is a member of the IEE, the Society for Neuroscience, and the Association for Research in Vision and Ophthalmology.